中國機械工程學刊第四十五卷第三期第 253~262 頁(民國一百一十三年)
Journal of the Chinese Society of Mechanical Engineers, Vol.45, No.3, pp253~262 (2024)

Design and Control System Research of Hydraulic Pressure Test Bench

Xu Fang*, Youmin Wang**and Lili Zhang*

Keywords: parameter identification, system operating pressure, control method, neural network

ABSTRACT

For the existing hydraulic pressure servo system test bench overall performance is poor. This paper takes the hydraulic pressure servo valve-controlled symmetric hydraulic cylinder closed-loop force control system as the research object. The design of the hydraulic control system and the calculation and selection of hydraulic components are completed. It is proposed to take the error force between the input and output of the system as the optimization objective to obtain the global optimal working pressure of the hydraulic system. To improve the accuracy of the system model, it is proposed to take the system response overshooting amount as the evaluation index. The design of the orthogonal test is analyzed to obtain the flow gain coefficient and stiffness damping ratio as the important parameters to be identified to affect the model accuracy. Based on Matlab, the system mathematical model is obtained by using least squares to identify the parameters. For the unsatisfactory effect of PID control, a BP-PID controller is designed. The adjustment time of the system is 0.02s, which is 96% higher than that of the traditional PID control, as obtained through simulation. It is verified through experiments that u_i, u_f, u_g, u are used as input signals. The BP-PID control system can output the optimal PID control parameters under this condition through the adjustment of the weights of each layer by the neural network. Realize the adaptive control of the hydraulic pressure servo control system.

Paper Received September, 2023. Revised January, 2024. Accepted February, 2024. Author for Correspondence:

** Graduate Student, School of Mechanical Engineering, Anhui Polytechnic University, Wuhu, Anhui 241000, China.*

*** Professor, School of Mechanical Engineering, Anhui Polytechnic University, Wuhu, Anhui 241000, China.*

INTRODUCTION

Hydraulic technology has a wide range of applications in the metallurgical industry, agricultural machinery, and aerospace industry (2021). At present, the domestic high-end hydraulic components production technology and hydraulic pressure servo test bench are relatively backward. This has become a bottleneck restricting the development of hydraulic technology in China. Therefore it is necessary to design a new hydraulic pressure servo test bench to enhance the level of research in hydraulics.

The performance of the hydraulic servo test bench mainly depends on the control system design. The traditional PID control regulator has good adaptability, and robustness and does not need to rely on the precise system model of the controlled object, so it is widely used. For the PID parameter tuning optimization problem, the traditional methods are the response curve method, expert method, Ziegler Nichols method (2020), ideal relay characteristics method, etc. With the development of hydraulic technology, a series of complex industrial process control devices and systems with large hysteresis, time-varying, time-lag, nonlinearity, etc. (2020). PID controllers are difficult to accurately regulate such complex and abstracted systems. At this stage the combination of fuzzy, genetic algorithm, particle swarm, neural network, and so on with PID. Zhu Z (2021), M. D A (2019), and Zhang F (2022) have used fuzzy PID control. The performance of a fuzzy PID control system depends on the selection of fuzzy rules and affiliation functions. This in turn depends heavily on the designer's knowledge of the control loop characteristics. Mingxue L (2021), Bai Tao (2022), and Liu Xiaojuan (2020) utilized the genetic algorithm PID control. The genetic algorithm has poor adaptability to the search space and is prone to premature convergence, which reduces the efficiency of PID parameter optimization. Woo S K (2015), and Zhao Yan (2023) used neural network PID control. As the neural network has the advantages of adaptive learning and robustness, it makes the overall control effect of the system better.

This paper focuses on the closed-loop force control system of a symmetrical hydraulic cylinder controlled by a servo valve in a hydraulic pressure servo test stand. Through experimental and theoretical research. The mathematical model of the control system is established, and the relevant parameters in the mathematical model are identified. Use the software to simulate the electro-hydraulic force servo test bench using different optimized control methods respectively. Compare the stability, response speed, control accuracy, and other indicators of the test bench system. Reasonable control parameters and optimal control methods are derived to improve the control performance of the system.

HYDRAULIC CONTROL SYSTEM DESIGN

To study the performance related to the hydraulic servo control system, the schematic diagram of the hydraulic control system was designed. It is shown in Fig. 1.

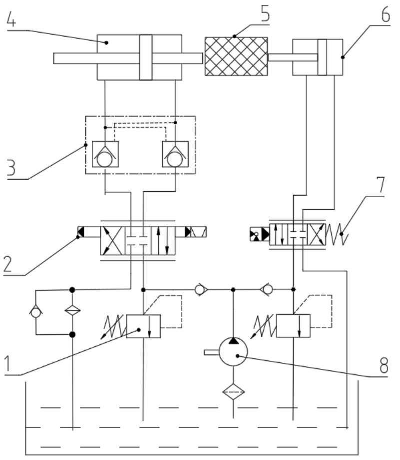

1-Relief valve 2-Electro-hydraulic servo valve 3-Hydraulic lock 4-Double-outlet hydraulic cylinder 5-Pressure sensing 6-Single-outlet hydraulic cylinder 7-Solenoid valve 8-Hydraulic pump

Fig. 1. Hydraulic control system schematic diagram

The hydraulic servo control system is mainly composed of electro-hydraulic servo valves, double-outlet hydraulic cylinders, and an oil supply system. The oil supply system includes an oil tank, oil supply circuit, and oil return circuit. The oil supply circuit includes an oil suction filter, quantitative pump, relief valve, hydraulic gauge assembly, and check valve.

In this paper, the rated pressure of the hydraulic system is set to 6MPa, the maximum load is 10KN, and the left and right stroke of the piston rod is 100mm. According to the existing research equipment in the laboratory, combined with the designed hydraulic control system schematic diagram. After calculating the selection of each component in the hydraulic system, the hydraulic control system component models are shown in Table 1.

Table 1. Models of hydraulic control system components for the test bench

Name	Parameters	Model
Hydraulic cylinder	D=63mm d=35mm	——
Hydraulic Pumps	——	CBGF1018 Gear Pumps
Electric motors	Power Rating 5.5kw	Y2-132S-4
Electro-hydraulic servo valve	Rated flow rate 20	4WSE2EM6-2X
One-way valve	Rated flow rate30	RVP10-30B
Servo Amplifier	——	NB2000
Relief valve	Rated flow rate 30L/min	DBDS6G10/200
Pressure sensors	Measurement range0~1000kg Voltage0~10V	Seamless steel pipe Inner diameter 16mm，Wall thickness2mm

Conventional hydraulic systems are constant pressure source systems where the system pressure is constant and the load pressure varies with the load. The load pressure of a hydraulic transmission system exceeding the maximum pressure of the system may lead to a dangerous runaway of the system. Therefore, it is necessary to satisfy the design criterion $P_L \leqq 2/3P_s$. For the servo valve to operate in a good linear operating range, the relief valve must produce an appropriate throttling pressure drop. To solve this conflict, the ideal control method is to adapt the relief valve operating pressure to the load pressure by adjusting the relief valve operating pressure. The optimal operating pressure of the system is found to ensure that the system can work safely and stably.

According to the preset maximum load force of the system, the maximum pressure of the hydraulic cylinder inlet is 4.25MPa. So the maximum working pressure of the hydraulic control system is 6.375MPa. To get the global optimal working pressure of the system, the simulation and analysis of electro-hydraulic servo control through AMESim software can be seen. When P_s>6.375MPa, the simulation data of the hydraulic cylinder and servo valve have no change. When P_s is 4.25~6.375MPa, the relevant performance of the hydraulic system shows obvious changes. Therefore, we focus on analyzing the relevant performance of the system when the working pressure of the relief valve is 4.25~6.375MPa.

Firstly, 4.25MPa~6.4MPa is divided into 11 points (4.246, 4.468, 4.684, 4.904, 5.122, 5.34, 5.558, 5.776, 5.994, 6.225, 6.375). The relief valve operating pressure is varied and different step signals are input. The error data of the input force and output force of the electro-hydraulic servo control system were obtained in Fig. 2. It can be seen that the system input force is below 2000N, and the relief valve operating pressure has almost no effect on the system. The system input force is in 2000~10000N. With the change of the relief valve working pressure, the error of the system shows obvious fluctuation. It is most obvious when the relief valve working pressure is at 4.25MPa. This is caused by the fact that the components of the hydraulic system will generate pressure loss, resulting in insufficient system pressure.

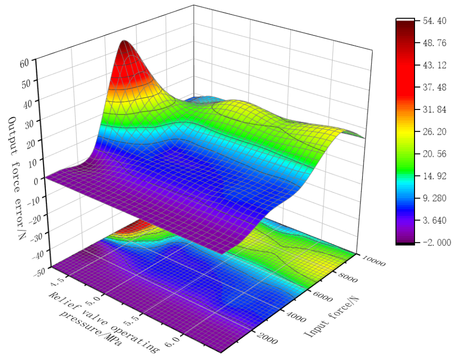

Fig. 2. 3D surface plot of system output force error

The data in the above table is further analyzed. The operating pressure of the relief valve is set as the x-axis and the cumulative error under different input forces is set as the y-axis. Processing the Fig.2 data yields 11 points for curve fitting using “Polynomial”. This is shown in Fig. 3. It can be seen that the relief valve pressure is 5.58 MPa when the system input and output are minimal. When the minimum error of input and output is used as the evaluation index, the global optimal working pressure of the hydraulic control system is obtained as 5.58MPa.

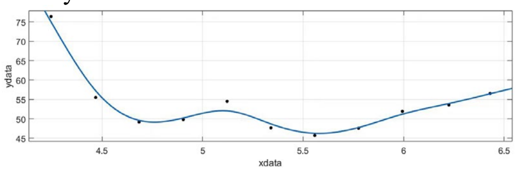

Fig. 3. System error curve fitting

ELECTRO-HYDRAULIC SERVO CONTROL SYSTEM MODELING

As the hydraulic system is characterized by distributed parameters, combined with the hydraulic control system designed in this paper. In this paper, the modular modeling method is used to model the system. The hydraulic pressure control scheme of the test bench is shown in Figure 4.

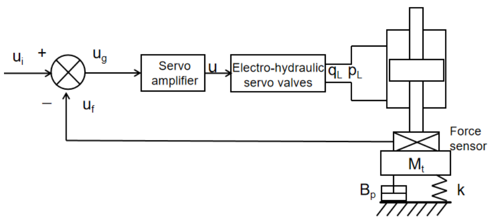

Fig. 4. Control scheme diagram of electro-hydraulic servo system

The existing theoretical studies and modeling methods of hydraulic servo control systems are relatively mature. However, the modeling process is more complicated and the model accuracy is not high. This paper proposes to use modular modeling, and the modeling process is mainly divided into three stages: dividing the subsystem, establishing the basic model, and aggregate modeling.

First of all, the subsystem division is carried out. In this paper, the valve-controlled symmetric cylinder control system is divided into three modules: control module, valve-controlled symmetric cylinder module, and feedback module.

Mathematical modeling of valve-controlled symmetric cylinder module

In an electrohydraulic servo system, it is assumed that there is no elastic load and the viscous damping coefficient is extremely small. The leakage flow due to viscous friction forms a piston velocity much lower than its motion, then the hydraulic cylinder transfer function can be divided into third-order links. The slide valve flow equation, the continuity equation of the hydraulic cylinder, and the force balance equation of the hydraulic cylinder can be listed to establish the hydraulic cylinder model.

In this paper, a three-position four-way zero-opening electro-hydraulic servo-slider valve is selected. Its linearized flow equation is:

$$q_L = K_q x_v - K_c p_L \tag{1}$$

$$K_q = \frac{\partial q_L}{\partial x_v} = C_d W \sqrt{\frac{1}{\rho}(p_s - p_L)} \tag{2}$$

$$K_c = -\frac{\partial q_L}{\partial p_L} = \frac{CdWxv\sqrt{\frac{1}{\rho}(p_s - p_L)}}{2(p_s - p_L)} \tag{3}$$

$$K_p = \frac{\partial p_L}{\partial x_v} = \frac{2(p_s - p_L)}{x_v} = \frac{K_q}{K_c} \tag{4}$$

The hydraulic cylinder continuity equation is an equation that describes the continuity of the fluid flow in a hydraulic cylinder. It is derived based on the law of conservation of mass and the principle of continuity. The continuity equation is:

$$q_L = A_p \frac{dx_p}{dt} + C_{tp} p_L + \frac{V_t}{4\beta_e}\frac{dp_L}{dt} \tag{5}$$

$$A_p p_L = m_t \frac{d^2 x_p}{dt^2} + B_p \frac{dx_p}{dt} + K x_p \tag{6}$$

The following equation is obtained by Rasch transformation:

$$\begin{cases} Q_L = K_q X_v - K_c P_L \\ Q_L = A_p s X_p + C_{tp} P_L + \dfrac{V_t}{4\beta_e} s P_L \\ A_p P_L = m_t s^2 X_p + B_p s X_p + K X_p \end{cases} \tag{7}$$

According to the above slide valve flow equation, cylinder flow continuity equation, hydraulic cylinder, and load force balance equation can be derived from the hydraulic cylinder transfer function as follows:

$$G_h(s) = \frac{\frac{K_{sv}}{A_p K_{ce}}(\frac{s^2}{\omega_m^2}+1)}{(\frac{s}{\omega_r}+1)(\frac{s^2}{\omega_h^2}+\frac{2\xi_h}{\omega_h}s+1)} \tag{8}$$

In the force servo control system studied in this paper. The electro-hydraulic servo valve responds quickly, and it is considered that the frequency of the servo valve is much larger than that of the hydraulic actuating element, and only the static performance is considered. So in this paper, the servo valve is directly regarded as a proportional link. Its expression is:

$$G_{sv}(s) = K \tag{9}$$

Feedback module

The system regards the pressure sensor as a proportional link. The range of the pressure sensor is 0 to 1000kg and the voltage is 0 to 10V. So the gain of the pressure sensor is:

$$K_{fF} = \frac{10V}{10000N} = 10^{-3}V/N \tag{10}$$

Other modules

According to the type of servo valve to determine its reasonable with the amplifier, select the appropriate amplifier category. The model number is NB2000, the supply voltage is 24DC, the power consumption is 25W, the maximum output current is 810mA, and the maximum load resistance is 30Ω. Then the gain of the servo amplifier is:

$$K_a = \frac{810mA}{24V} = 33.75mA/V \tag{11}$$

Based on the known model of the subsystem and the boundary conditions of the division. The aggregate model of the whole system is built according to certain rules. The mathematical model of the system is:

$$G(s) = \frac{K_a K_{sv}\frac{K_q}{K_{ce}}A_p K_{fF}(\frac{s^2}{\omega_m^2}+1)}{\left(\frac{s}{\omega_r}+1\right)(\frac{s^2}{\omega_h^2}+\frac{2\xi_h}{\omega_h}s+1)} \tag{12}$$

PARAMETER IDENTIFICATION

The performance of hydrodynamic servo systems is affected by the manufacturing tolerances of the geometry of control valves, spools, hydraulic cylinders, pressure sensors, and the leakage and friction coefficients. This results in a number of physical quantities that are difficult to determine during the modeling process of electro-hydraulic servo control systems. Although it is possible to derive the relevant parameters of the transfer function based on the modeling process using traditional calculation formulas. However, with the wide application of hydraulic systems, so it is necessary to identify the relevant parameters of the system model.

In this paper, the transfer function of the electro-hydraulic servo control system of the test bench is obtained through modular modeling. The system transfer function to be recognized is:

$$G(s) = \frac{K_a K_{sv}\frac{K_q}{K_{ce}}A_p K_{fF}(\frac{s^2}{\omega_m^2}+1)}{\left(\frac{s}{\omega_r}+1\right)(\frac{s^2}{\omega_h^2}+\frac{2\xi_h}{\omega_h}s+1)} \tag{13}$$

Observing the above transfer function, there are many parameters to be identified, which causes complexity and difficulty in the identification process. To reduce the difficulty of identifying the parameters. This paper proposes to use orthogonal experiments first. By analyzing the degree of influence of each parameter on the size of the system model through the polar deviation, the parameters that are most necessary for identification are judged.

In this paper, valve gain, flow gain coefficient, flow-pressure coefficient, stiffness damping ratio, and hydraulic cylinder intrinsic frequency are selected as the five factors of this orthogonal test. As shown in Table 2. They are denoted by A, B, C, D, and E, respectively. The orthogonal test of this design has four levels, i.e., five factors and four levels of orthogonal test. The evaluation indexes selected are the amount of overshoot and response time of the system model under the action of the stop signal. According to the selection of factors and levels. It can be seen that this test is a five-factor four-level test, so $L_{16}(4^5)$ is the most appropriate.

Table 2. Orthogonal test factor level table

Factors	A (Ksv)	B (Kq)	C (Kce)	D (Wr)	E (Wh)
Level 1	8	7	6.4	0.168	214
Level 2	11.11	10	9.4	0.268	244
Level 3	14	13	12.4	0.368	274
Level 4	17	16	15.4	0.468	30

To analyze the extent of influence of each experimental factor on the accuracy of the model. According to the 16 groups of different parameters listed in the orthogonal table, the mathematical models of the 16 groups of data were obtained using Matlab programming. Simlink software was used to simulate the mathematical models of the 16 groups of data. The simulation results are shown in Table 3.

Table 3. Orthogonal test table and results

Serial number	A (Ksv)	B (Kq)	C (Kce)	D (Wr)	E (Wh)	Over shoot (%)
1	8	7	6.4	0.186	214	0.503
2	8	10	9.4	0.286	244	0.609
3	8	13	12.4	0.386	274	0.666
4	8	16	15.4	0.486	304	0.704
5	11.11	7	9.4	0.386	304	0.658
6	11.11	10	6.4	0.486	274	0.820
7	11.11	13	15.4	0.186	244	0.515
8	11.11	16	12.4	0.286	214	0.703
9	14	7	12.4	0.486	244	0.710
10	14	10	15.4	0.386	214	0.700
11	14	13	6.4	0.286	304	0.811
12	14	16	9.4	0.186	274	0.734
13	17	7	15.4	0.286	274	0.575
14	17	10	12.4	0.186	304	0.604
15	17	13	9.4	0.486	214	0.866
16	17	16	6.4	0.386	244	0.889

Combined with the 16 sets of experimental data obtained from the statistical table of simulation results. Polar analysis was used to explore the effect of each parameter of the model on the maximum overshoot. The results of the analysis are shown in Table 4..

Table 4. Extreme variance analysis table

	A	B	C	D	E
K1	2.482	2.446	3	2.356	2.772
K2	2.696	2.733	2.867	2.698	2.723
K3	2.955	2.858	2.683	2.913	2.795
K4	2.934	3.03	2.494	3.1	2.777
k1	0.6205	0.6115	0.75	0.589	0.693
k2	0.674	0.68325	0.71675	0.6745	0.68075
k3	0.73875	0.7145	0.67075	0.72825	0.69875
k4	0.7335	0.7575	0.6235	0.775	0.69425
R	0.11825	0.146	0.1265	0.186	0.018

The magnitude of the extreme variance is used to judge the extent to which the test factor affects the results of the test. The larger the extreme variance, the greater the influence on the results. According to the extreme difference analysis table can be seen. The two factors of flow gain coefficient and hydraulic cylinder intrinsic frequency have the greatest influence on the modeling accuracy of the system and need to be identified as parameters.

After clarifying the parameters to be recognized in the electro-hydraulic servo control system, the experiments are designed by combining the a priori knowledge. Through the preliminary collection and processing of experimental data. Use the identification algorithm to identify the model parameters, and carry out qualified calibration of the identified mathematical model. Cycle the above steps until a model structure that can be equivalent to the actual system performance is found. The identification process is shown in Fig. 5.

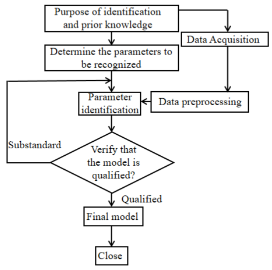

Fig. 5. Flowchart for model parameter identification

In this paper, offline identification combined with a least squares identification algorithm is used to identify the electro-hydraulic servo control system. According to the research above. The model to be recognized is in the form of a fifth-order, two-unknown parameter transfer function with the transfer function:

$$G(s)=\frac{K_q(107.74s^2+8.62\times10^4)}{\left(\frac{s}{\omega_r}+1\right)\left(\frac{1}{59536}s^2+1.64\times10^{-3}s+1\right)}$$

To perform system parameter identification, a series of experiments are first designed to obtain the input and output data of the system. In designing the experiments, the type and range of input signals need to be considered. Examples are step signals, sinusoidal signals, or other excitation signals. The experiments should cover the operating range of the system and make sure that the input signals vary over a large enough range of amplitude and frequency.

First of all, it is necessary to obtain the data to be recognized as system-related data. In this paper, Amesim software is used to build a model of the electro-hydraulic force servo system of the test bench, and “random” is selected as the signal source of the system simulation. Through the setup, 1002 groups of step signals are generated randomly in 10s, and their values range from 0 to 10000null. Through the simulation of the system actuator feedback signal. The simulation model is shown in Fig. 6.

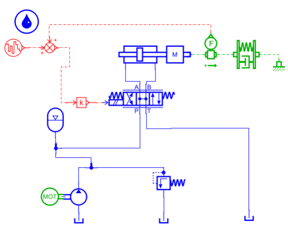

Fig. 6. Simulation model

The input signal of the system model and the output force signal of the hydraulic cylinder are shown in Fig. 7.

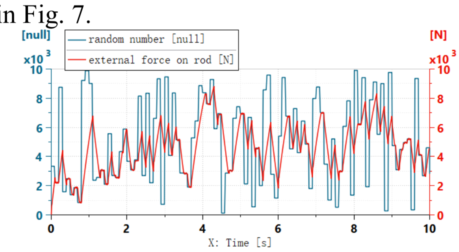

Fig. 7. Simulation data

The input and output simulation data obtained from Amesim are imported into Matlab “workspace”. the start time is set to 0. The sampling time is set to 0.01 according to the simulation time and simulation interval in Amesim. the output and input data are obtained as shown in Fig. 8.

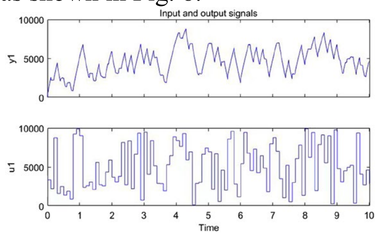

Fig. 8. Input and Output Signal Plot

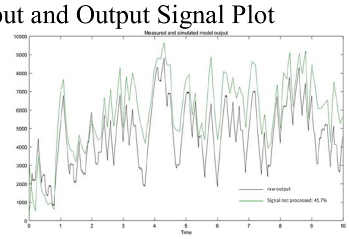

Fig. 9. Data Fitting Plot

Figure 9 shows the data fitting graph, it can be seen that the fit is not satisfactory, only 45.7% and the input signal needs to be preprocessed to improve the fit to be recognized. Select "Select range" to process the data, the first 5s for model identification, and the last 5s for data validation, as shown in Figure 10.

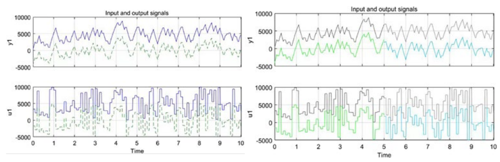

(a) (b)

Fig. 10. Data Processing Chart

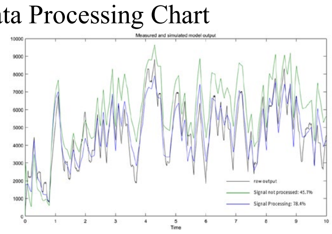

Fig. 11. Plot of data fit

After signal preprocessing, the data fitting plot is shown in Figure 11. The fit of the to-be-identified parameter data is 78.4%, which is a significant improvement. The parameters to be identified Kq-flow gain coefficient is 3.78×10^{-5} and the Wr-stiffness damping ratio is 0.277. The transfer function of the system is obtained as follows

$$G(s)=\frac{5.92\times10^{-2}s^{2}+3.26}{6.02\times10^{-5}s^{3}+5.92\times10^{-2}s^{2}+1.64\times10^{-3}s+1)}$$

RESEARCH ON CONTROL METHODS

PID control

PID control is widely used because of its simple structure and easy parameter adjustment. PID parameter adjustment is generally chosen as an empirical trial parameter method. The parameters of the PID controller are selected as $K_p=9$、$K_i=0.9$ and $K_d=0.2$ respectively by empirical trial parameters.

The PID control step response curve of the system using Simulink simulation is shown in Fig. 12. The performance of the system with PID control gets some improvement. When a unit step signal is input, the system reaches a steady state in 0.9s. However, the system's fast response is accompanied by a certain amount of overshoot, which needs to be improved and optimized.

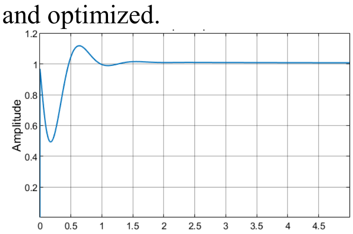

Fig. 12. PID control step response curve

BP-PID control

The optimization of PID controller parameters based on the BP neural network to control the hydraulic pressure servo system gives the hydraulic pressure servo system the ability of self-adaptation and autonomous learning. The working principle of its BP-PID controller is as follows: input force signal ui, deviation signal ug, feedback signal uf, and servo amplifier output signal u are used as inputs to the BP neural network. After the training and learning of the neural network, the three parameters Kp, Ki, and Kd of the PID controller are obtained. Then the PID controller output signal is amplified by the servo amplifier to control the output flow of the electro-hydraulic servo valve, thus controlling the output force of the double-outlet hydraulic cylinder. The control principle is shown in Fig. 13.

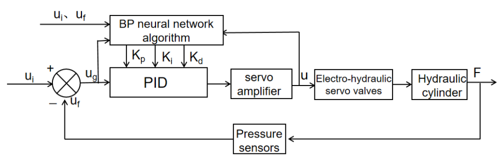

Fig. 13. Neural network PID control schematic diagram of hydraulic pressure servo control test bench.

Neural networks can improve the control error accuracy by increasing the number of network layers and the number of neurons in the hidden layer. Considering that too many neural network layers can lead to a complex programming process. Appropriately increasing the number of neurons in the hidden layer, on the contrary, makes the network training effect easier to observe and adjust. So priority is given to increasing the number of neurons in the hidden layer. The number of neurons is selected according to the following formula.

$$s_1 = \sqrt{S+S_2} + (1 \sim 10) \tag{16}$$

In this paper, a three-layer BP neural network is used. As shown in Figure 14, the number of neurons in the input layer is 4, respectively ui, uf, ug, u. The number of neurons in the output layer is 3, respectively, for the three parameters of the PID controller Kp, Ki, Kd. The number of neurons in the hidden layer is 12.

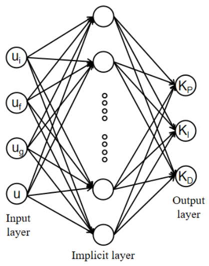

Fig. 14. Structure of BP neural network.

The activation function of the BP neural network must be everywhere minimizable, generally using logarithmic, hyperbolic tangent, and linear functions [23, 24]. Considering the 3 parameters of the PID controller must be positive. So the nonlinear logistic function is used for the output layer activation function and the tanh-type hyperbolic tangent function is used for the hidden layer.

$$\log istic(x) = \frac{1}{1+e^{-x}} \tag{17}$$

$$\tan ch(x) = \frac{e^{x}-e^{-x}}{e^{x}+e^{-x}} \tag{18}$$

Fig. 13 Schematic diagram of the control system contains the classical PID controller and the neural network controller. Take ui, uf, ug, u as neural network inputs. Through the self-learning of the neural network, the weight coefficients are adjusted so that the neural network outputs the optimal PID control parameters. Then the PID controller controls the hydraulic pressure servo system, thus realizing the optimal and stable operation of the system. The specific algorithm is as follows.

The classical PID control equation is:

$$\begin{aligned} \mathrm{u}(k) &= u(k-1) + K_p[u_g(k) - \\ & u_g(k-1)] + K_I u_g(k) + \\ & K_D[u_g(k) - 2u_g(k-1) + u_g(k-2)] \end{aligned} \tag{19}$$

The output of the kth neuron of the hidden layer is:

$$a_{1\mathrm{k}} = f_1(\sum_{j=1}^{r} \omega_{1\mathrm{k}j} p_j + b_{1\mathrm{k}})(\mathrm{k}=1,2,3...,12) \tag{20}$$

The output of the zth neuron of the output layer is:

$$W_z = f_2(\sum_{k=1}^{s_1} \omega_{2kj} a_{1k} + b_{2z})(z=1,2,3) \tag{21}$$

The error function is:

$$E(W,B) = \frac{1}{2}\sum_{z=1}^{3}(t_z - W_z)^2 \tag{22}$$

The weight coefficients are updated using the gradient descent method for the weight coefficients of the output and hidden layers [25].

The weights from the ith input to the kth output of the output layer are:

$$\Delta\omega_{2ki} = -\eta\frac{\partial E}{\partial \omega_{2ki}} = \eta(t_k - W_k)\frac{\partial W_k}{\partial u(k)} f'_2 a_{1i}$$
$$= \eta\delta_{ki}a_{1i}$$
(23)

The weights of the jth input to the ith output of the implicit layer are:

$$\Delta\omega_{1\mathrm{ij}} = -\eta\frac{\partial E}{\partial \omega_{1\mathrm{ij}}} = \eta(t_k - W_k) f'_2 \omega_{2\mathrm{ij}} f'_1 \mathrm{p}_j$$
$$= \eta\delta_{ij}p_j$$
(24)

By designing and analyzing the BP-PID controller and algorithm. Matlab programming is used to realize the simulation control of BP-PID on the hydraulic pressure servo control system test bench. The following figure shows the BP neural network regulating PID to get the specific Kp, Ki, and Kd parameters.

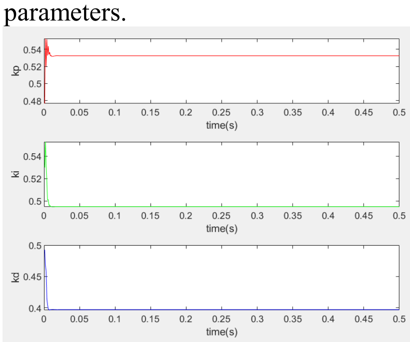

Fig. 15. Neural network output parameter plot

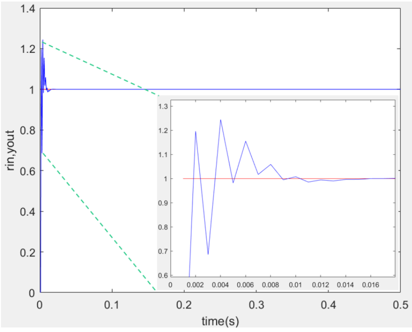

Fig. 16. BP-PID step response plot

Fig. 15 Neural network output parameters Kp=0.53, Ki=0.49, Kd=0.39. Fig. 16 shows the step response curve of BP-PID, and the overtime ts is only 0.02 s. It can be seen that, after the introduction of the BP neural network, the BP-PID controller can effectively output Kp, Ki, and Kd. Although the amount of overshoot has not been significantly reduced, the tuning time of BP-PID is shortened by 0.75s compared with the traditional PID control. The system response is greatly improved. When the load outside the hydraulic servo control system is changed. The control system can adjust the weights of each layer by the BP neural network through the feedback of the error so that its output is the optimal PID control parameter under the condition. Realize the hydraulic pressure servo control system adaptive control.

EXPERIMENT

According to the hydraulic control system components selection table, complete the electro-hydraulic servo control system test bench and related testing experiments. The test bench is shown in Figure 17.

Fig. 17. General assembly of the test stand

Fig. 18 shows the response curve obtained by using the traditional PID controller for the test rig. The input force is 5000 N. The adjustment time for the system to reach a steady state is 0.8s, and the overshoot is large. Figure 19 shows the test bench using the BP-PID controller designed in this paper. The test bench input force signal, deviation signal, pressure sensor feedback signal, and servo amplifier output signal as the inputs of the BP-PID controller. The output response curve of the test bench is obtained in real-time. The input force is 5000N, and the adjustment time for the system to reach a steady state is 0.4s, with a slight decrease in the overshooting amount.

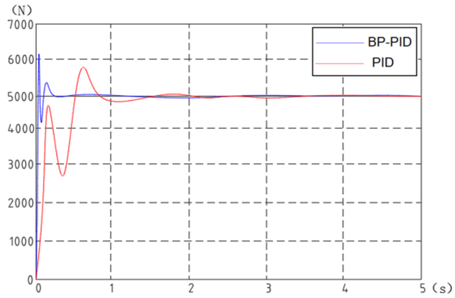

Fig. 18. PID and BP-PID control system response graph

CONCLUSION

The design of the hydraulic control system and the calculation and selection of hydraulic components were completed. The error force between the input and output of the system is proposed as the optimization target. The optimal working pressure of the hydraulic system is obtained as 5.58MPa.

After the mechanism analysis, this paper adopts modular modeling. Aiming at the model with too many unknown parameters makes the identification process difficult. Proposed to the system response overshooting amount as an evaluation index. Through the orthogonal test analysis of the flow gain coefficient, the stiffness damping ratio is an important parameter to be identified to affect the accuracy of the model. Based on Matlab, we use least squares to identify the parameters to obtain an accurate model of the hydraulic servo control system.

Aiming at the unsatisfactory effect of PID control, a BP-PID controller is designed. It is derived through simulation when Kp=0.53, Ki=0.49, Kd=0.39. The adjustment time of the system unit step response is 0.02s, which is 96% higher than the traditional PID control. A test bench is built, and ui, uf, ug, u are used as input signals. the BP-PID control system can be adjusted by a neural network for the weights of each layer. The real-time optimal PID control parameter combination under this condition is derived. Adaptive control of the hydraulic pressure servo control system is realized.

AUTHOR CONTRIBUTIONS

Xu Fang made substantial contributions to design, experimental research, data collection, and result analysis; Youmin Wang and Lili Zhang made critical changes to important academic content.

DATA AVAILABILITY

The data used to support the findings of this study are included within the article.

CONFLICTS OF INTEREST

The authors declare that they have no conflicts of interest to report regarding the present study.

REFERENCES

Bai T. "Cloud model PID hydraulic bending roller plate shape control based on genetic algorithm optimization" [J]. Journal of Plasticity Engineering, 2021, 28(04):206-211.

Cococcioni M,Rossi F,Ruffaldi E, et al. "Fast Approximations of Activation Functions in Deep Neural Networks when using Posit Arithmetic" [J]. Sensors, 2020, 20(5).

HOU Yuanxin, Fan Jiuchen. "Research on active lift and sink compensation predictive control of hydraulic drive with neural network PID control" [J]. Machine Tools and Hydraulics, 2020, 48(16):145-148+200.

Jin Ying, Ning Chuming, Han Shousong et al. "Control characterization of single-degree-of-freedom hydraulic test bench based on Fuzzy-PID" [J]. Machine Tools and Hydraulics, 2021, 49(17):147-150.

Juxian Zhang,Wei Liu. "Research on prediction of strong earthquake roadbed collapse deformation by BP neural network algorithm considering activation function" [J]. Journal of Earthquake Engineering, 2019, 41(02): 406-411+475.

Jianbo W, Liang C, Yingjie G, et al. "Dynamic modeling and parameter identification for a gantry-type automated fiber placement machine combined with hydraulic balance system and nonlinear friction" [J]. CIRP Journal of Manufacturing Science and Technology, 2022, 37.

Li Huanjun, Zhang Yimin. "Fluid lubrication characteristic test system and principle of piston pump sliding shoe" [J]. Journal of Xi'an Jiaotong University, 2021, 55(08):9-17.

Liu Xiaojuan, Xia Yundong, Li Gang et al. "Simulation analysis of control of hydraulic machinery volumetric speed control system based on GA optimized PID algorithm" [J]. Forging and pressing technology, 2022, 47(03):164-168.

Liu Shengfei, Sun Qinglin, Chen Zengjian et al. "Antidisturbance commutation hysteresis compensation backstepping control for proportional valve-controlled electrohydraulic systems" [J]. Control Theory and Applications, 2020, 37(07):1521-1534.

Linjun Jin, Jianan Fang, Leining Pan. "A neural network PID controller based on improved particle swarm optimization algorithm" [J]. Mechanical and Electrical Engineering, 2015, 32(02):295-300.

Mingzheng Tang, Chuang Li, Rongnian Tang. "Fractional order PID~(μ) controller based on Ziegler-Nichols rectification rule" [J]. Control Engineering: 1-8 [2023-09-01].

M. D A,N. K,S. K N. "Fuzzy Fractional-Order PID Controller for Fractional Model of Pneumatic Pressure System" [J]. Mathematical Problems in Engineering, 2018, 2018.

Mingxue L,Guolai Y,Xiaoqing L, et al. "Variable Universe Fuzzy Control of Adjustable Hydraulic Torque Converter Based on Multi-Population Genetic Algorithm"[J]. IEEE Access, 2019, 7.

Napole C, Barambones O, Calvo I, et al. "Feedforward compensation analysis of Hebb learning rule-based artificial neural network, Hebb learning rule-based artificial neural network and single neuron PID piezoelectric actuator" [J]. Energy, 2020, 13(15).

Qingsong W, Haoyu X, Fujin D, et al. "Design and analysis of genetic algorithm and BP neural network based PID control for boost converter applied in renewable power generations" [J]. IET Renewable Power Generation, 2021, 16(7).

Ruqi D, Xueshan M, Min C, et al. "Terminal force soft sensing of hydraulic manipulator based on the parameter identification" [J]. Measurement, 2022, 200.

Wei M, Linfang Q, Longmiao C. "Hydraulic node model and parameter identification of a dull recoil brake" [J]. Journal of Mechanical Science and Technology, 2022, 36(11).

Woo S K, Buyoun C,Seunghoon S, et al. "Force Control of a Hydraulic Actuator With a Neural Network Inverse Model" [J]. IEEE ROBOTICS AND AUTOMATION LETTERS, 2021, 6(2).

Xu F, Youmin W, Bo Z. "Research on the Control Method of Force Servo System of Liquid Hydrostatic Guide Oil Film Thickness Test Bench for Machine Tools" [J]. Shock and Vibration, 2022, 2022.

Zhang F, Zong S, Li X, et al. "Hydraulic gap control of rolling mill based on self-tuning fuzzy PID" [J]. Journal of Intelligent & Fuzzy Systems, 2016, 31(6).

Zhu Z, Lu X, Lei J, et al. "Nonlinear Dynamic Analysis Based Fuzzy PID Control Approach for Complex Hydraulic Driving Process" [J]. International Journal of Precision Engineering and Manufacturing, 2018, 19(7).

Zhao Yan, Zhou Qinyuan, Shao Nianfeng et al. "Electrohydraulic servo system based on fuzzy PID control with RBF neural network" [J]. Mechanical and Electrical Engineering, 2022, 39(02):244-249.

Zeng Yonglong, Zhao Xiaobin, Deng Pan et al. "Research on adaptive variable gap sealing technology of ultra-high pressure piston hydraulic cylinder" [J]. Machine Tools and Hydraulics, 2022, 50(02):122-126.

Zhang Q, Xiong W, Wang H, et al. “Research on modular modelling for the hydraulic system of a vehicle shift” [J]. The Journal of Engineering, 2019, 2019(13).

NOMENCLATURE

P_L the load pressure

X_v the Spool displacement of slide valves

K_q the Flow Gain

K_c the Pressure-flow coefficient

Ap the Effective working area of hydraulic cylinder

xp the Hydraulic Cylinder Displacement

C_{tp} the Total leakage factor for hydraulic cylinders

V_t the Total compressed volume

β_e the Effective bulk modulus of elasticity

m_t the Load quality

B_p the Load damping factor

K the Load spring stiffness

K_{mn} the sum of evaluation indicators corresponding to the mth factor at the nth level

Q_{mn} the values of evaluation indicators corresponding to the mth factor at the nth level

K_{mn} the mean value of evaluation indicators corresponding to the mth factor at the nth level.

R_m the extreme difference value of the mth factor

K_{max} the Maximum value of the average value of the evaluation indicators corresponding to the mth factor at all levels

K_{max} theminimum value of the average value of evaluation indicators corresponding to all levels of the mth factor.

液壓力試驗台設計及控制系統研究

方旭 王幼民 張麗麗
安徽工程大學機械工程學院

摘 要

本文研究液壓力伺服閥控對稱液壓缸的閉環力控制系統;完成了液壓控制系統設計及液壓元件的計算選型;爲了使伺服閥工作處在線性區間,提出以系統輸入與輸出的誤差力作爲優化目標,溢流閥産生適當的節流壓降,得到液壓系統最優工作壓力;考慮到液壓控制系統理論分析研究比較完善和成熟,經過機理分析本文采用模塊化建模,爲了提高模型精度,提出以系統響應超調量作爲評價指標,通過正交試驗分析得出流量增益系數、剛度阻尼比爲影響模型精度的重要待辨識參數,基于 matlab 采用最小二乘對參數進行辨識;針對 PID 控制效果不理想,設計 BP-PID 控制器,通過仿真得出系統的調整時間爲 0.02s,較傳統 PID 控制提高了 96%,通過試驗驗證,以 u_i、u_f、u_g、u 作爲輸入信號,BP-PID 控制系統可以通過神經網絡對各層權值的調整,輸出該條件下最優的 PID 控制參數,實現液壓力伺服控制系統自適應控制。